Supporting Information

Influence of the co-Ligand on the Magnetic and Relaxation Properties of Layered Co(II) Thiocyanato Coordination Polymers

Susanne Wöhlert, Zbigniew Tomkowicz, Michal Rams, Stefan Ebbinghaus, Lothar Fink, Martin U. Schmidt and Christian Näther

Corresponding Author: Christian Näther (cnaether@ac.uni-kiel.de)

Contents

	2000 Oe	
Tables S3-S4	Results of the fitting procedure of $\chi_{AC}(f)$ dependences for $[Co(NCS)_2(bpe)]_n$.	18

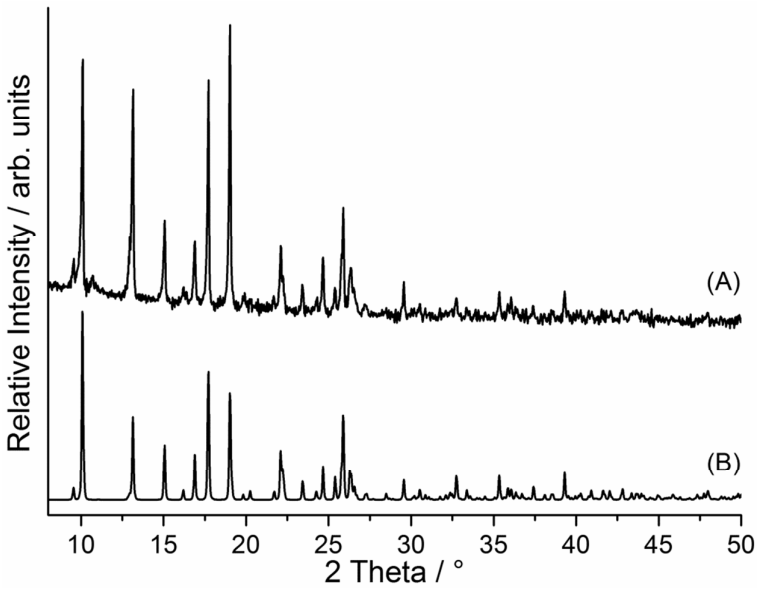

Figure S1. Experimental XRPD (A) and calculated XRPD (B) of $[Co(NCS)_2(bpa)_2]_n$.

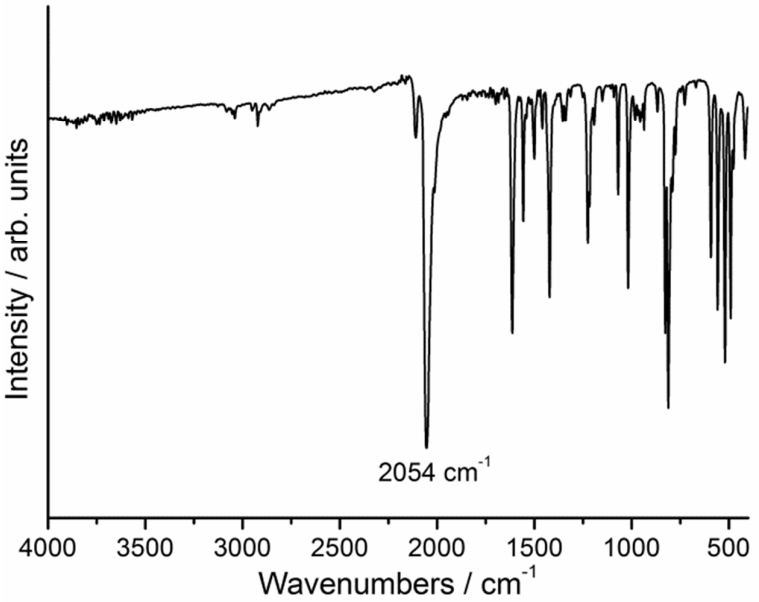

Figure S2. IR spectrum of $[Co(NCS)_2(bpa)_2]_n$. IR (ATR): ν_{max} = 2054 (s), 1613 (m), 1556 (m), 1499 (m), 1458 (w), 1420 (m), 1353 (w), 1341 (w), 1224 (m), 1192 (w), 1068 (m), 1017 (m), 981 (w), 955 (w), 935 (w), 866 (w), 826 (m), 810 (s), 592 (m), 557 (m), 520 (m), 490 (m), 416 (m) cm^{-1}.

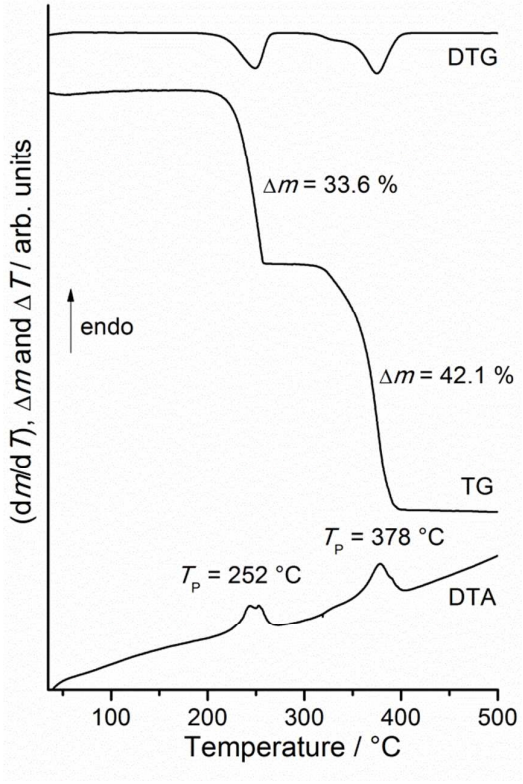

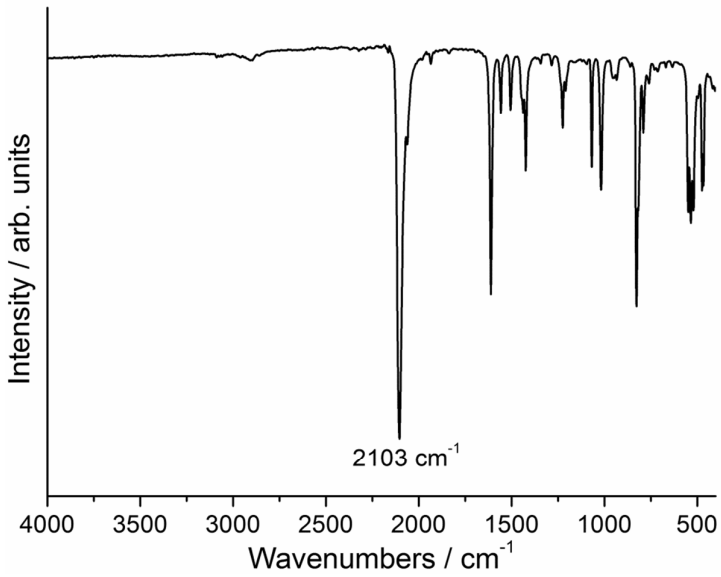

Figure S3. Top: DTG, TG and DTA curve for $[Co(NCS)_2(bpa)]_n$. Heating rate = 4°C/min; the peak temperatures T_P in °C and the mass loss in % are given. Bottom: IR spectrum of $Co(NCS)_2$(4-bpa). IR (ATR): ν_{max} = 2103 (s), 1610 (m), 1558 (w), 1505 (w), 1437 (w), 1423

(m), 1224 (m), 1067 (m), 1017 (m), 954 (w), 934 (w), 826 (m), 791 (m), 548 (m), 534 (m), 474 (m) cm^{-1}.

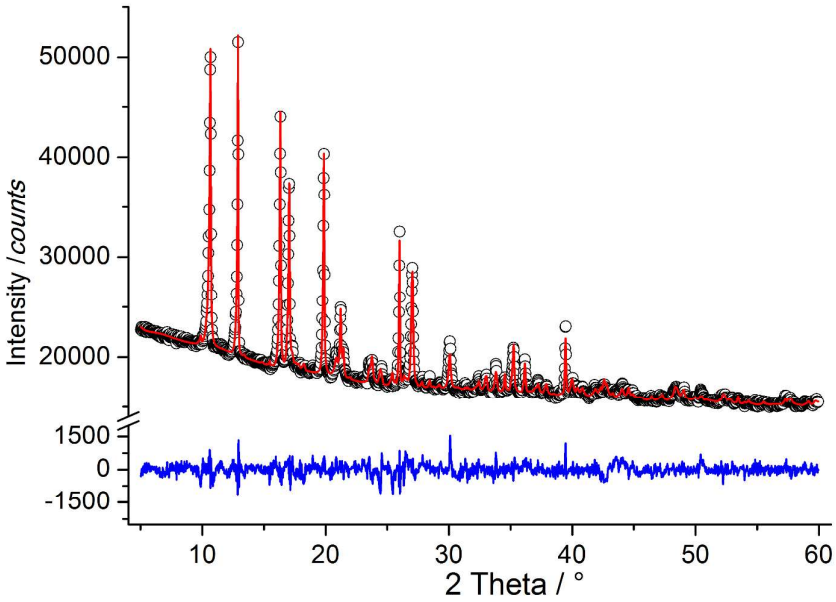

Figure S4. Rietveld plot of $[Co(NCS)_2(bpa)]_n$. Experimental data are drawn as points, calculated as through line, differences curve below. The vertical lines represent the reflection positions.

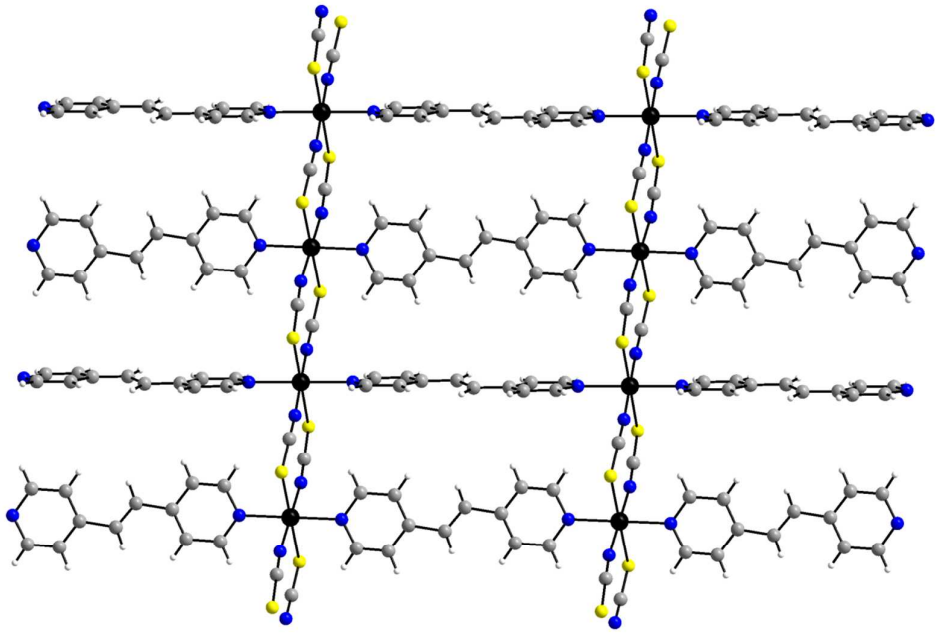

Figure S5. Crystal structure of $[Co(NCS)_2(bpe)]_n$ retrieved from literature (see text in manuscript).

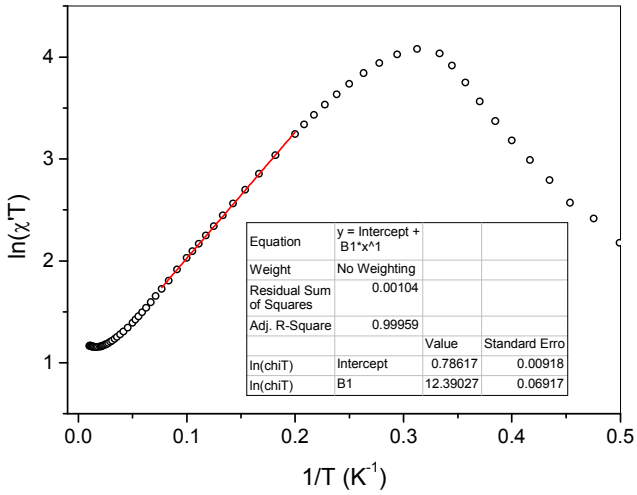

Figure S6. Plot of ln($\chi'T$) versus $1/T$ dependence for $[Co(NCS)_2(bpa)]_n$. The slope obtained with DC field of 100 Oe was 12.2 K.

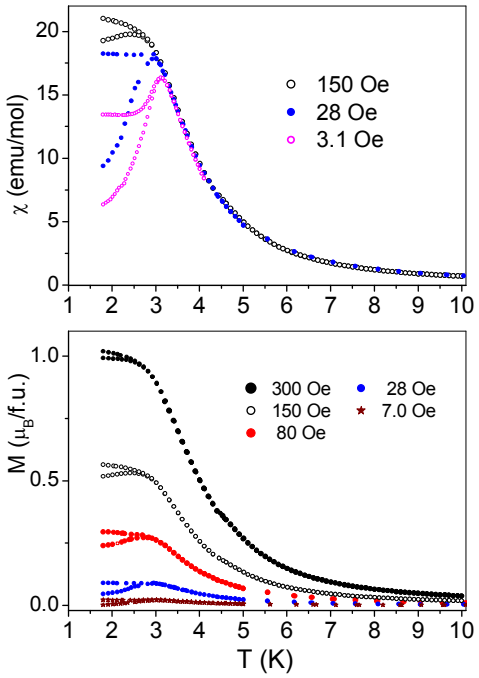

Figure S7. Temperature dependence of the magnetic susceptibility of $[Co(NCS)_2(bpa)]_n$ measured in FC and ZFC regime and plotted for three different magnetic field strengths 150, 28 and 3.1 Oe (upper panel). FC/ZFC temperature dependent magnetic moment plotted for various magnetic field strengths (300÷7 Oe) (lower panel).

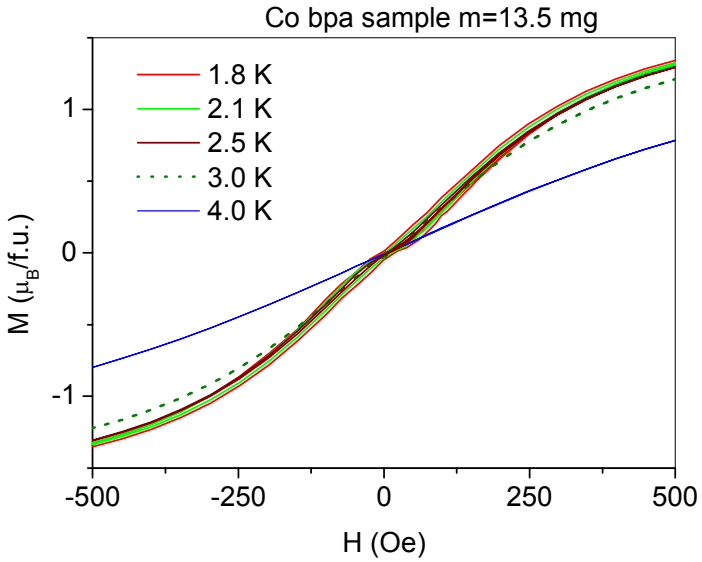

Figure S8. Field dependent magnetization curves for $[Co(NCS)_2(bpa)]_n$ at different temperatures.

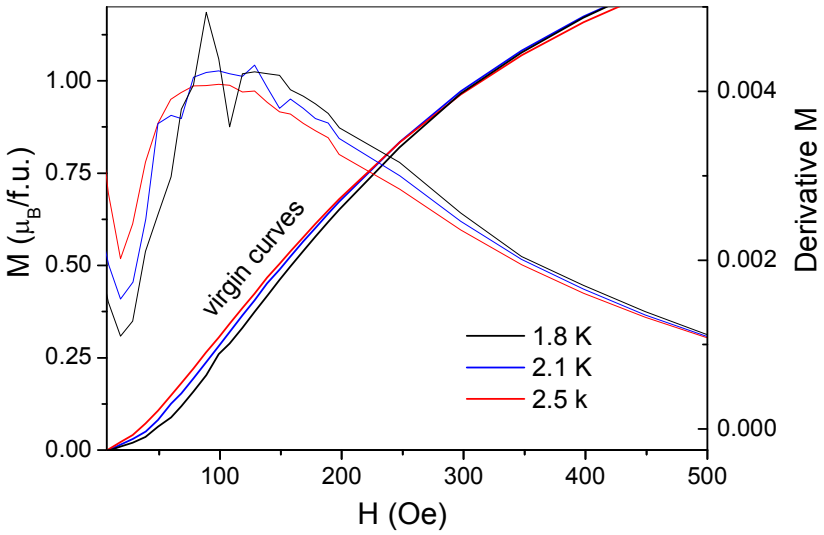

Figure S9. Field dependent magnetization and $\partial M/\partial H$ curves for $[Co(NCS)_2(bpa)]_n$ at different temperatures.

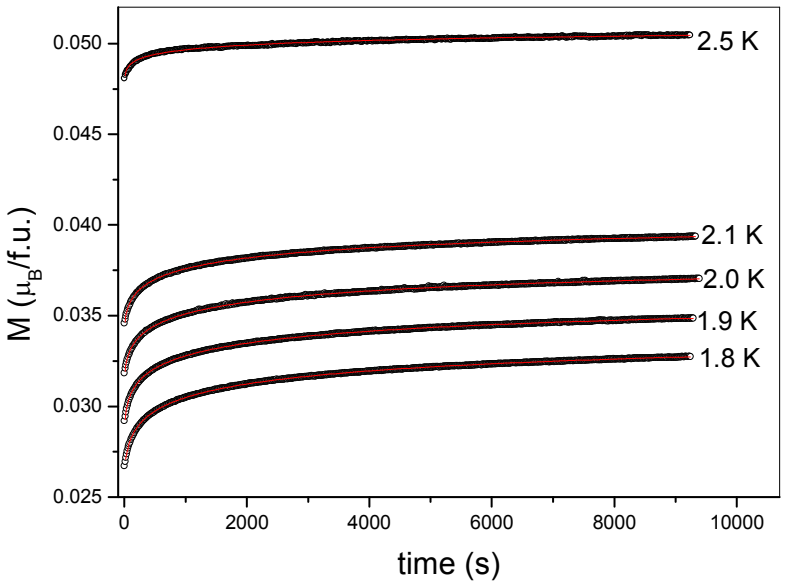

Figure S10. Time dependence of magnetization measured for $[Co(NCS)_2(bpa)]_n$ for zero field cooled sample after switching the field 30 Oe on.

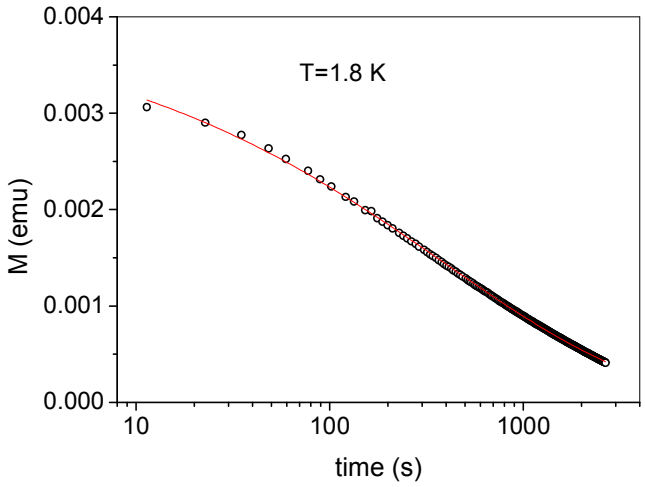

Figure S11. Time dependence of the magnetization measured for $[Co(NCS)_2(bpa)]_n$ according to the following procedure: field 100 Oe was set at 5 K, then the sample was cooled to 1.8 K, field was of and measurement started.

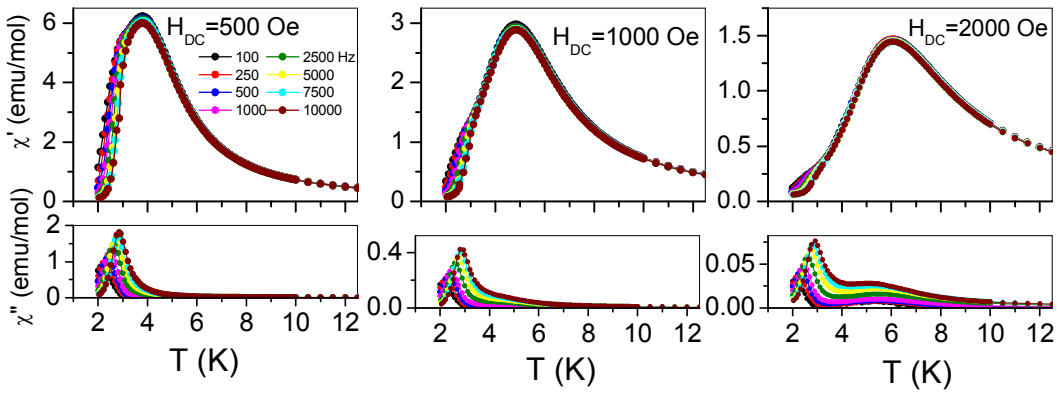

Figure S12. Temperature dependent AC susceptibility of $[Co(NCS)_2(bpa)]_n$ sample measured for various frequencies in three different DC bias magnetic fields. Amplitude H_{ac}=5 Oe.

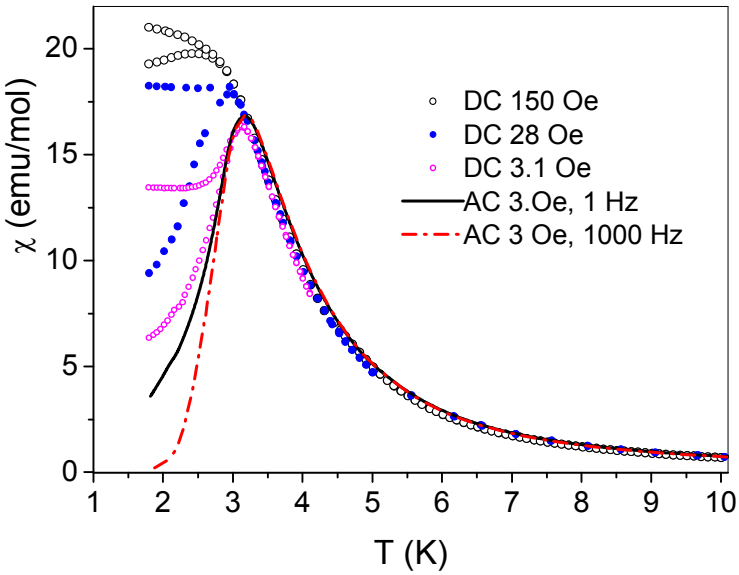

Figure S13. Comparison of temperature dependencies of DC and AC in phase susceptibility measured as a function of temperature for $[Co(NCS)_2(bpa)]_n$. DC susceptibility is plotted for three magnetic fields and AC susceptibility is plotted for zero DC field and 3 Oe amplitude of AC driving field for two frequencies.

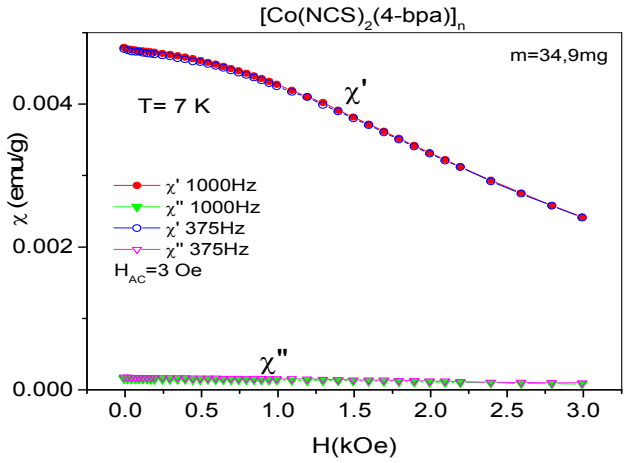

Figure S14. Field dependence of χ' and χ' for two different frequencies at 7 K for $[Co(NCS)_2(bpa)]_n$.

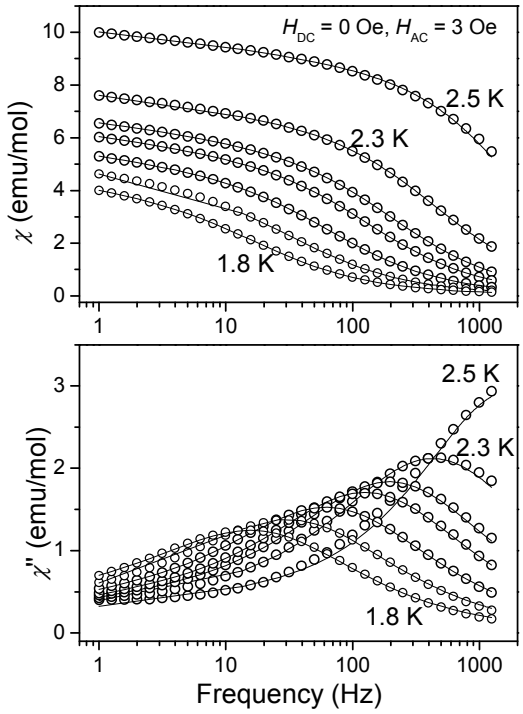

Figure S15. AC susceptibility of $[Co(NCS)_2(bpa)]_n$ measured as function of frequency at various temperatures for 0 Oe DC bias field. Solid lines are fits.

Table S1. Results of the fitting procedure for $[Co(NCS)_2(bpa)]_n$. H_{DC} = 0 Oe, H_{AC} = 3 Oe, fitting with two modes

T (K)	χ_0	$\chi_{\infty 1}$	χ_∞	τ_1(s)	α_1	τ_2(s)	α_2	χ^2
2.5	10.73	7.97	0	$8.77\cdot10^{-5}$	0.24	$8.78\cdot10^{-3}$	0.65	$3.90\cdot10^{-3}$
2.3	8.33	6.36	0	$3.48\cdot10^{-4}$	0.29	$4.25\cdot10^{-2}$	0.57	$4.47\cdot10^{-4}$
2.2	7.25	5.51	0	$7.47\cdot10^{-4}$	0.30	$5.84\cdot10^{-2}$	0.52	$1.75\cdot10^{-4}$
2.1	6.73	5.10	0	$1.15\cdot10^{-3}$	0.29	$7.07\cdot10^{-2}$	0.49	$1.14\cdot10^{-4}$
2.0	6.07	4.57	0	$2.29\cdot10^{-3}$	0.30	$1.09\cdot10^{-1}$	0.47	$4.57\cdot10^{-5}$
1.9	5.59	3.85	0	$4.43\cdot10^{-3}$	0.29	$1.26\cdot10^{-1}$	0.51	$5.02\cdot10^{-5}$
1.8	5.18	3.19	0	$8.28\cdot10^{-3}$	0.29	$1.53\cdot10^{-1}$	0.53	$5.99\cdot10^{-5}$

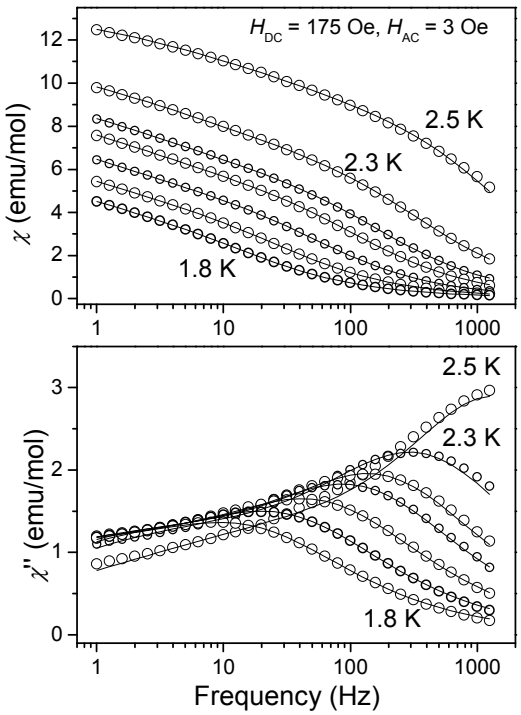

Figure S16. AC susceptibility of $[Co(NCS)_2(bpa)]_n$ measured as function of frequency at various temperatures for 175 Oe DC bias field. Solid lines are fits.

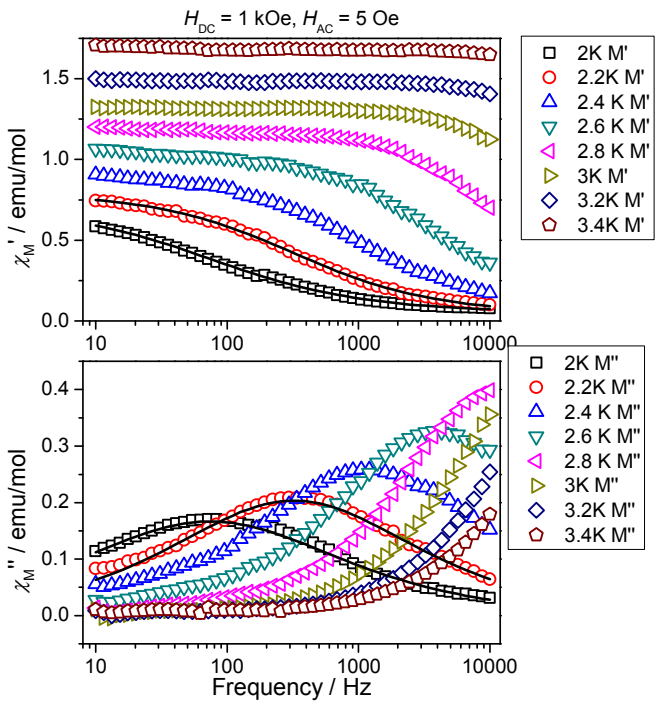

Figure S17. AC susceptibility of $[Co(NCS)_2(bpa)]_n$ measured as function of frequency at various temperatures for 1000 Oe DC bias field. Solid line through the data for 2.0 and 2.2 K are exemplary fits.

Table S2. Results of the fitting procedure for $[Co(NCS)_2(bpa)]_n$ H_{DC}=1000 Oe, Hac=5 Oe. Only one process is present.

T (K)	χ_0	χ_∞	τ_1(s)	α_1	χ^2
3.4	1.68	0	$1.63\cdot10^{-6}$	0.06	$3.02\cdot10^{-5}$
3.2	1.49	0	$2.64\cdot10^{-6}$	0.09	$2.47\cdot10^{-5}$
3.0	1.32	0	$5.13\cdot10^{-6}$	0.13	$4.46\cdot10^{-5}$
2.8	1.19	0	$1.26\cdot10^{-5}$	0.23	$6.26\cdot10^{-5}$
2.6	1.06	0	$3.74\cdot10^{-5}$	0.31	$8.24\cdot10^{-5}$
2.4	0.93	0.006	$1.33\cdot10^{-4}$	0.37	$7.38\cdot10^{-5}$
2.2	0.80	0.04	$4.95\cdot10^{-4}$	0.38	$4.22\cdot10^{-5}$
2.0	0.72	0.05	$2.13\cdot10^{-3}$	0.41	$2.52\cdot10^{-5}$

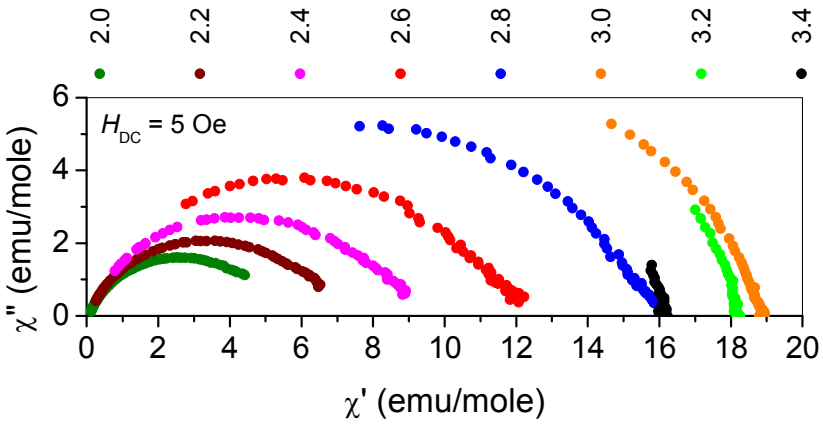

Figure S18. Argand plots for $[Co(NCS)_2(bpa)]_n$ in the bias DC field of 5 Oe obtained with PPMS in the frequency range 10-10000 Hz.

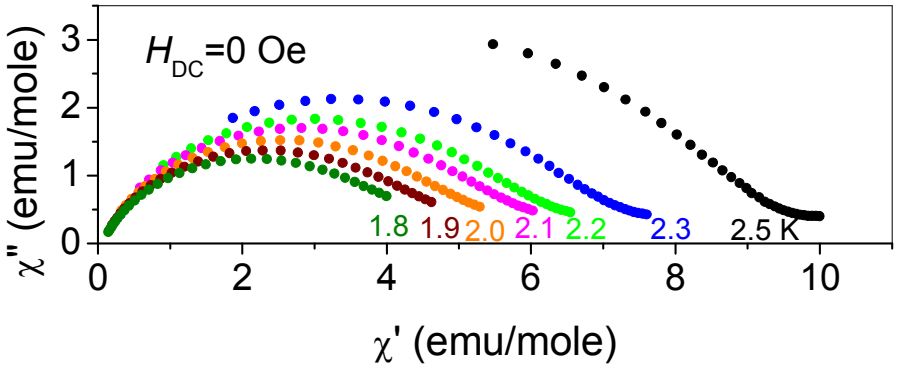

Figure S19. Argand plost for $[Co(NCS)_2(bpa)]_n$ in the bias DC field of 0 Oe obtained with SQUID in the frequency range 1-1000 Hz.

.

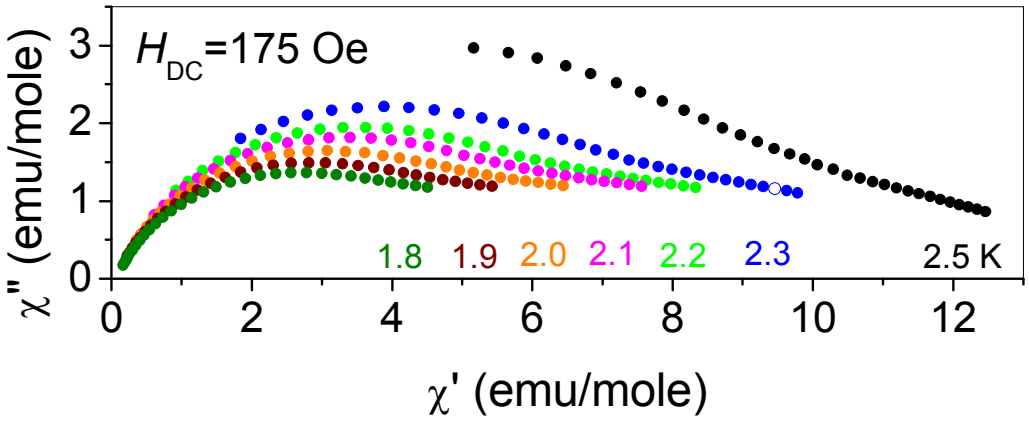

Figure S20. Argand plots for $[Co(NCS)_2(bpa)]_n$ in the bias DC field of 175 Oe and in the frequency range 1-1000 Hz.

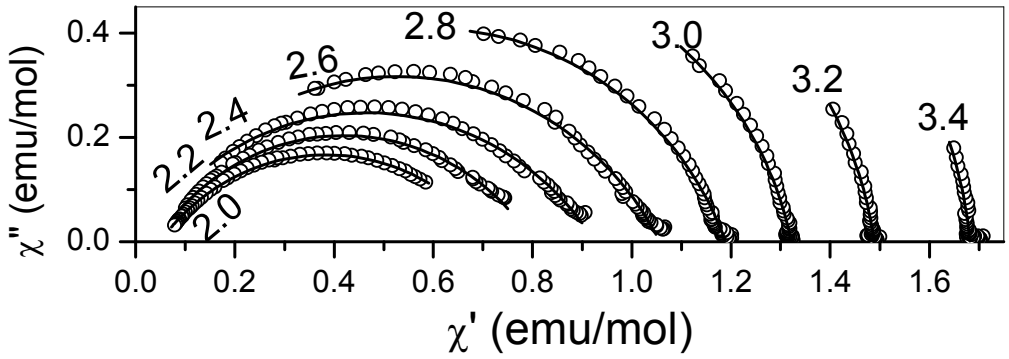

Figure S21. Argand plots for $[Co(NCS)_2(bpa)]_n$ in the bias DC field of 1000 Oe and in the frequency range 10-10000 Hz. Lines are fits with one relaxation process.

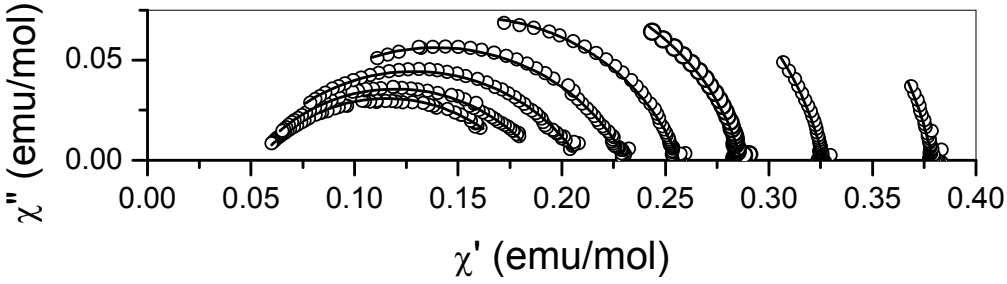

Figure S22. Argand plots for $[Co(NCS)_2(bpa)]_n$ in the bias DC field of 2000 Oe and in the frequency range 10-10000 Hz. Lines are fits with one relaxation process.

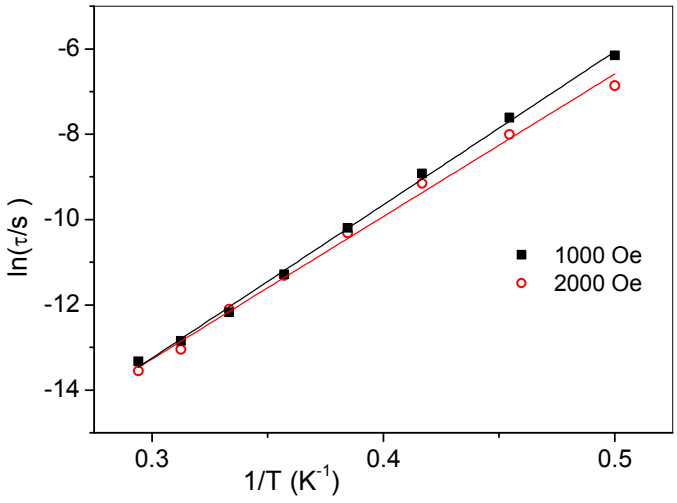

Figure S23. Dependence of ln τ vs. $1/T$ in 1000 and 2000 Oe bias field for $[Co(NCS)_2(bpa)]_n$. Lines are linear fitsc

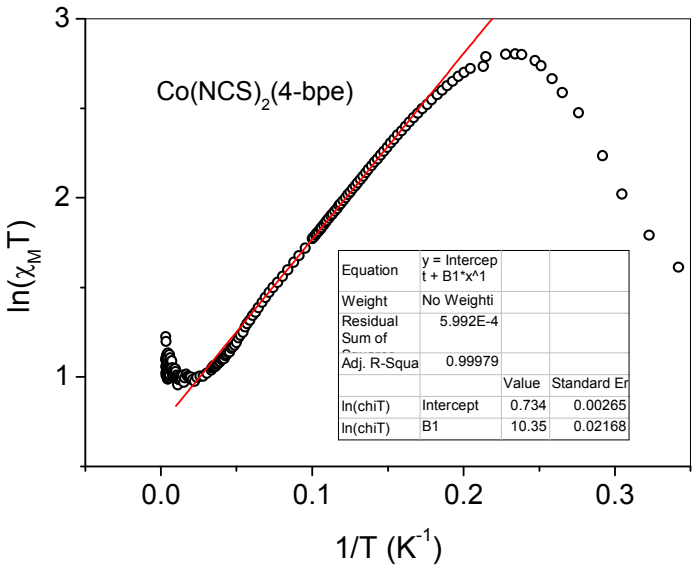

Figure S24. Plot of $\ln(\chi_M T)$ versus $1/T$ for $[Co(NCS)_2(bpe)]_n$ in field of 100 Oe. χ_M is molar susceptibility in emu units.

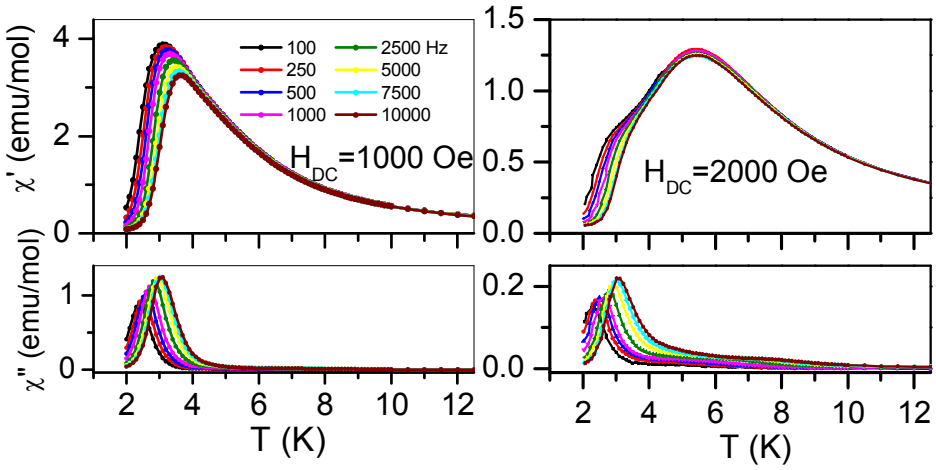

Figure S25. Temperature dependent AC susceptibility measured for $[Co(NCS)_2(bpe)]_n$ at various frequencies in two bias DC magnetic fields.

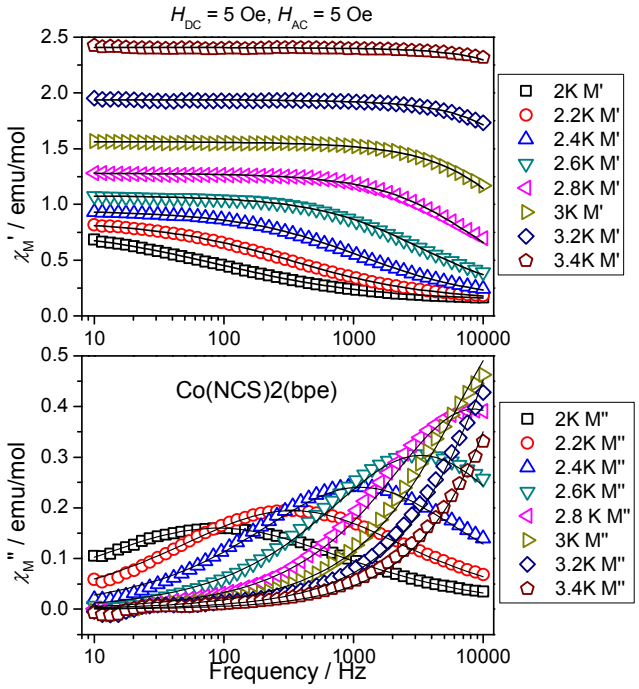

Figure S26. AC susceptibility of $[Co(NCS)_2(bpe)]_n$ measured as function of frequency at various temperatures for 5 Oe DC bias field. Solid lines are fits.

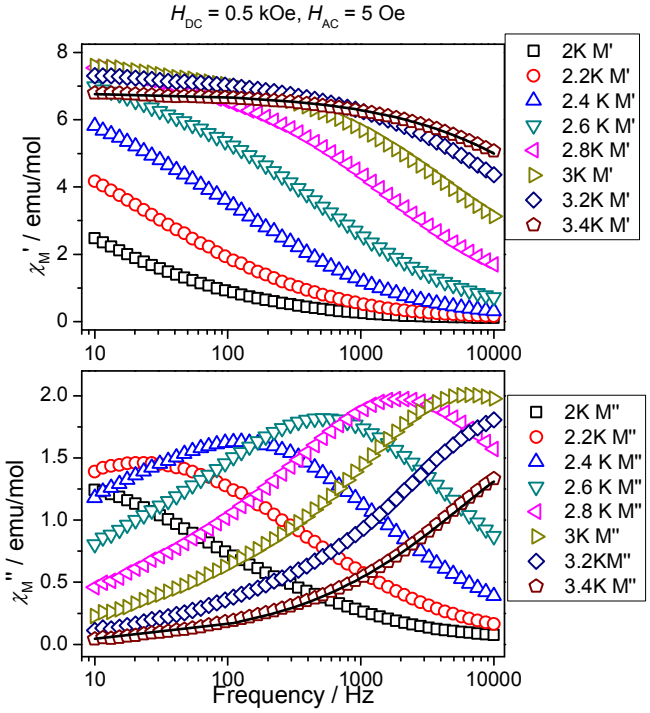

Figure S27. AC susceptibility of $[Co(NCS)_2(bpe)]_n$ measured as function of frequency at various temperatures for 500 Oe DC bias field. Solid line through the data for 3.4 K is an exemplary fit.

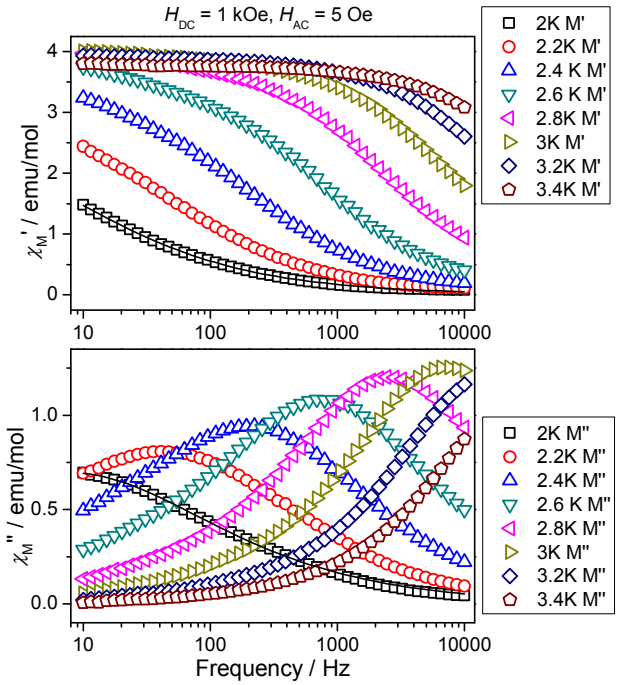

Figure S28. AC susceptibility of $[Co(NCS)_2(bpe)]_n$ measured as function of frequency at various temperatures for 1000 Oe DC bias field. Solid line through the data for 2.0 K is the fit.

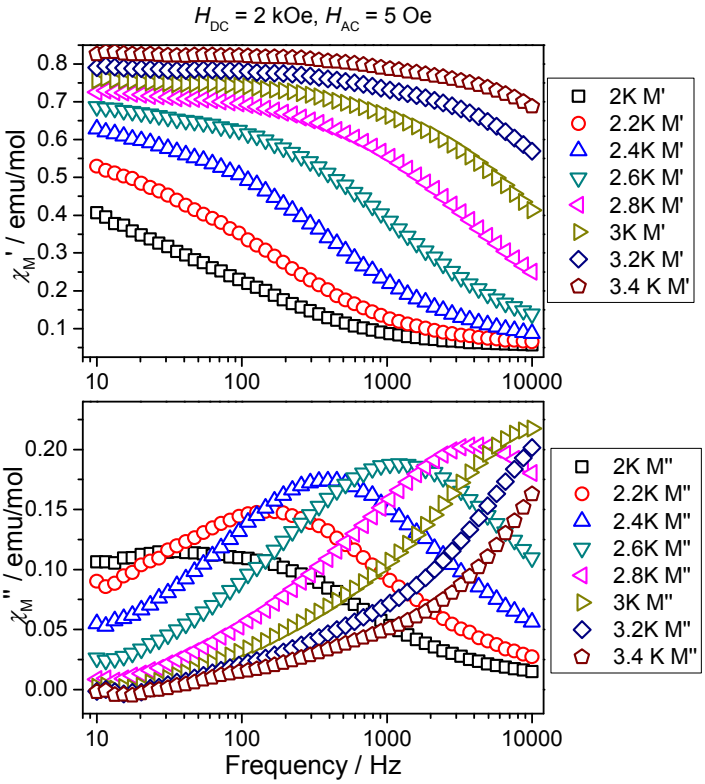

Figure S29. AC susceptibility of $[Co(NCS)_2(bpe)]_n$ measured as function of frequency at various temperatures for 2000 Oe DC bias field.

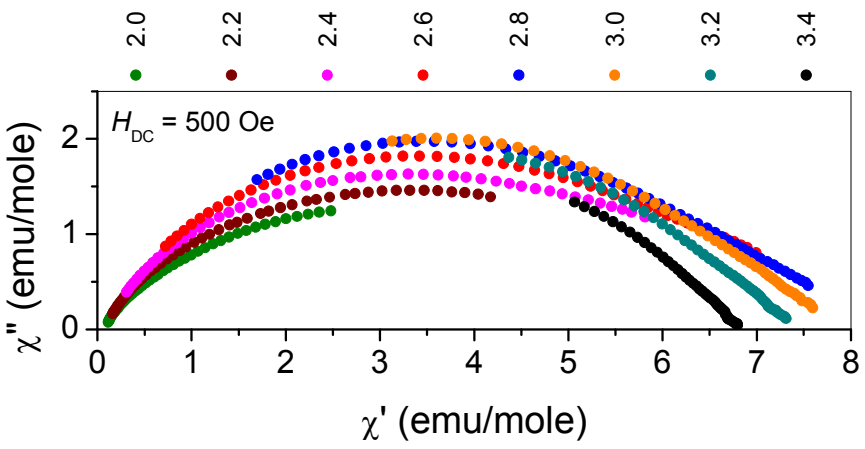

Figure S30. Argand plots for $[Co(NCS)_2(bpe)]_n$ corresponding to bias magnetic fields of 500 Oe

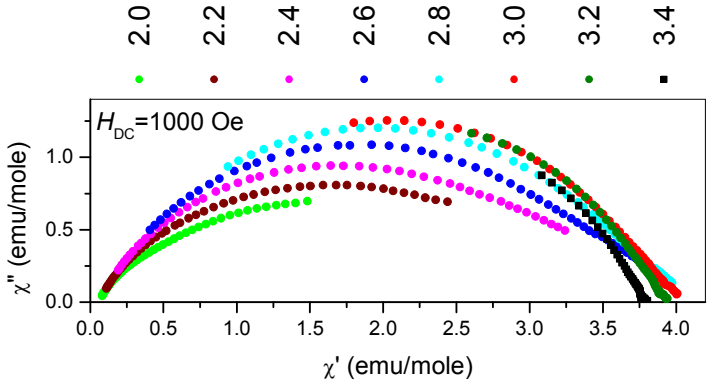

Figure S31. Argand plots for $[Co(NCS)_2(bpe)]_n$ corresponding to bias magnetic fields of 1000 Oe

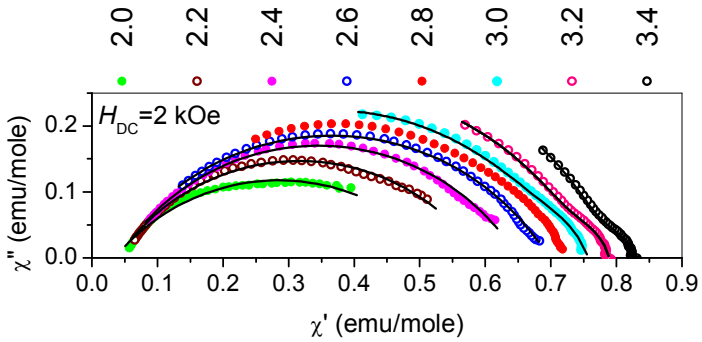

Figure S32. Argand plots for $[Co(NCS)_2(bpe)]_n$ corresponding to bias magnetic fields of 2000 Oe. Solid lines are fits.

Table S3. Results of the fitting procedure for $[Co(NCS)_2(bpe)]_n$. H_{DC}=5 Oe, H_{AC}=5 Oe.

T (K)	χ_0	χ_∞	τ_1(s)	α_1	χ^2
3.4	2.41	0	$2.07\cdot10^{-6}$	0.10	$5.77\cdot10^{-5}$
3.2	1.94	0	$3.76\cdot10^{-6}$	0.13	$5.98\cdot10^{-5}$
3.0	1.56	0	$7.07\cdot10^{-6}$	0.19	$9.03\cdot10^{-5}$
2.8	1.28	0.15	$1.90\cdot10^{-5}$	0.22	$8.83\cdot10^{-5}$
2.6	1.08	0.14	$4.84\cdot10^{-5}$	0.27	$6.79\cdot10^{-5}$
2.4	0.95	0.13	$1.41\cdot10^{-4}$	0.32	$3.57\cdot10^{-5}$
2.2	0.86	0.13	$4.73\cdot10^{-4}$	0.38	$1.31\cdot10^{-5}$
2.0	0.79	0.13	$1.76\cdot10^{-3}$	0.46	$3.67\cdot10^{-5}$

Table S4. Results of the fitting procedure for $[Co(NCS)_2(bpe)]_n$. H_{DC}=0.5 kOe, H_{AC}=5 Oe,.

T (K)	χ_0	$\chi_{\infty1}$	χ_∞	τ_1(s)	α_1	τ_2(s)	α_2	χ^2
3.4	6.83	2.15	0	$3.01\cdot10^{-6}$	0.06	$6.20\cdot10^{-6}$	0.47	$1.56\cdot10^{-4}$
3.2	7.41	3.62	0	$6.57\cdot10^{-6}$	0.21	$3.11\cdot10^{-5}$	0.50	$2.77\cdot10^{-3}$
3.0	7.82	4.80	0	$1.74\cdot10^{-5}$	0.28	$1.90\cdot10^{-4}$	0.50	$3.22\cdot10^{-3}$
2.8	8.07	5.80	0	$6.27\cdot10^{-5}$	0.34	$1.63\cdot10^{-3}$	0.48	$4.35\cdot10^{-3}$
2.6	7.98	5.54	0	$2.17\cdot10^{-4}$	0.36	$5.75\cdot10^{-3}$	0.43	$1.62\cdot10^{-3}$
2.4	7.47	4.29	0	$6.28\cdot10^{-4}$	0.36	$1.03\cdot10^{-2}$	0.41	$2.51\cdot10^{-4}$
2.2	6.30	3.72	0	$2.5\cdot10^{-3}$	0.40	$2.03\cdot10^{-2}$	0.30	$9.28\cdot10^{-5}$
2.0	5.63	0	0	$2.29\cdot10^{-2}$	0.47	–	–	$1.13\cdot10^{-4}$